SPECTROSCOPIC STUDIES OF $M_x[Pt(CN)_4] \cdot yH_2O$*

Hartmut Yersin and Günter Gliemann

Institut fur Chemie
Universität Regensburg
8400 Regensburg, Germany

INTRODUCTION

Square planar $[Pt(CN)_4]^{2-}$ complexes tend to crystallize in columnar structures. The distances between the molecular units along the columnar axis are short, compared with the separations from column to column. This structure type is expected to exhibit some interesting physical properties. One compound ($K_2[Pt(CN)_4]Br_{0.3} \cdot 3.2H_2O$(KCP · $X_{0.3}$)) of the relatively large series of the tetracyanoplatinates has become famous mainly because of its extremely anisotropic conductivity.[1-3] However, most members of the tetracyanoplatinates are nonconducting compounds. This might be the reason why these have not attracted as many scientific investigations.

TABLE 1 shows a list of the tetracyanoplatinates (MCP) which crystallize in columnar structures. The Pt-Pt-distances R in the direction of the column can be varied according to the choice of the cations M and/or the crystal water content y from R = 3.67 Å to 3.09 Å. This allows the "adjustment" of the intermolecular interaction in the direction of the chains over a large range. This adjustment by the chemical substitution method, however, is discontinuous. Application of high pressure, on the other hand, permits "tuning" the in-chain interaction to any intermediate value. Consequently, the spectroscopic properties can be tuned continuously, as well.

The purpose of the present paper is, first, to summarize recent results found by spectroscopic investigations with polarized light under ambient conditions, at high pressure, and at low temperature. A correlation between the transition energies and structural properties is pointed out. Mainly R-dependent trends are discussed, and the results of an electronic band structure calculation are presented. In the second part of the paper the influence of the immediate surrounding on the $[Pt(CN)_4]^{2-}$ columns is discussed. For this purpose, rare earth cations (e.g. $M = Sm^{3+}$) with energy levels near the excited column states are used as "probe" ions. *Energy transfer* from the tetracyanoplatinate columns (donors) to Sm^{3+} (acceptor) is observed. Thus, a new system for energy-transfer investigations is presented that exhibits interesting aspects because of the tuneability of the donor states.

POLARIZED SPECTROSCOPY

The optical spectroscopy represents an appropriate method for investigating the physical properties of the tetracyanoplatinates(II), since the dominant transi-

*Manuscript received June 16, 1977.

0077-8923/78/0313-0539 $1.75/1

TABLE 1

TETRACYANOPLATINATES WITH DIFFERENT METAL-METAL-DISTANCES IN THE DIRECTION OF THE COLUMNS (AT ROOM TEMPERATURE)

$M_x[Pt(CN)_4] \cdot yH_2O$ (MCP)	Pt-Pt-distance R [Å]	Reference
$Na_2[Pt(CN)_4] \cdot 3H_2O$	3.67	4
$Sr[Pt(CN)_4] \cdot 5H_2O$	3.60	5
$Cs_2[Pt(CN)_4] \cdot H_2O$*	3.54	6
$K_2[Pt(CN)_4] \cdot 3H_2O$	3.48	7
$Rb_2[Pt(CN)_4] \cdot 1.5H_2O$	3.42	8
$Ca[Pt(CN)_4] \cdot 5H_2O$	3.38	5
$Sm_2[Pt(CN)_4]_3 \cdot 18H_2O$	3.35†	36
$K_2Sr[Pt(CN)_4]_2 \cdot 6H_2O$	3.33	5
$Ba[Pt(CN)_4] \cdot 4H_2O$	3.32	4, 5, 9
$(NH_4)_2[Pt(CN)_4] \cdot 2H_2O$	3.26	10
$KNa[Pt(CN)_4] \cdot 3H_2O$	3.25	10
$KLi[Pt(CN)_4] \cdot 2H_2O$	3.20	11
$Y_2[Pt(CN)_4]_3 \cdot 21H_2O$	3.18	12
$Mg[Pt(CN)_4] \cdot 7H_2O$	3.15	5
$Sr[Pt(CN)_4] \cdot 3H_2O$	3.09	5
$K_2[Pt(CN)_4]Br_{0.3} \cdot 3.2H_2O$ ($KCP \cdot X_{0.3}$)	2.89	13

*Helix structure.
†Spectroscopic estimate.

tions of these compounds lie in the energy range between the near ultraviolet and the infrared. Further, most of the spectroscopic properties such as oscillator strengths, transition energies, and emission properties, including lifetime, show a very anisotropic behavior, as is expected for the columnar structure type. Therefore, important additional information is gained if methods of *polarized* spectroscopy are applied.

Spectroscopic Properties under Ambient Conditions

An investigation of the properties of the tetracyanoplatinates requires the application of various methods of optical spectroscopy. The transitions that are polarized with the electric field vector **E** parallel to the columnar axis (c-axis) have extremely high oscillator strengths. These are therefore appropriately investigated by single-crystal reflectivity measurements.[19] The transitions polarized with $\mathbf{E} \perp c$, on the other hand, are relatively weak and should be detected by single-crystal absorption techniques. All the tetracyanoplatinates (II) exhibit a very strong emission. Consequently, the measurements of the polarized emission represent a further important source of information.

FIGURE 1 shows the polarized emission spectra of some tetracyanoplatinate(II) single crystals with different in-chain Pt-Pt-distances R. The spectra are recorded under ambient conditions (295°K, 1 atm) with **E** parallel and perpendicular to the chain axis, respectively. All the compounds show two differently polarized

transitions. It is seen from FIGURE 1 that the emission properties change systematically with a variation of R:

The transitions shift to lower energy with decreasing R. This effect is attributed to a decrease of the band-gap energy caused by an increase of the in-chain interaction. For further discussion see ENERGY BANDS.

The relative intensities $I(\mathbf{E} \parallel c)/I(\mathbf{E} \perp c)$ invert with reduction of R. A similar inversion of the relative intensities is observed with temperature decrease and can be understood in a first approximation applying a Boltzmann distribution to the two emitting states (*Low-Temperature Investigations*).

FIGURE 2 summarizes the peak energies of the emission and reflectivity spectra versus R^{-3}. The experimental data follow a R^{-n} power law[17,18] (with $n = 3.0 \pm 0.3$).

Reflectivity and emission peak energies with $\mathbf{E} \parallel c$ undergo the same red shift with decreasing R (constant Stokes shift), because they are connected with the same interband transitions. These are fully allowed (very high oscillator strengths) and can be assigned to transitions between one-electron hybrid molecular states

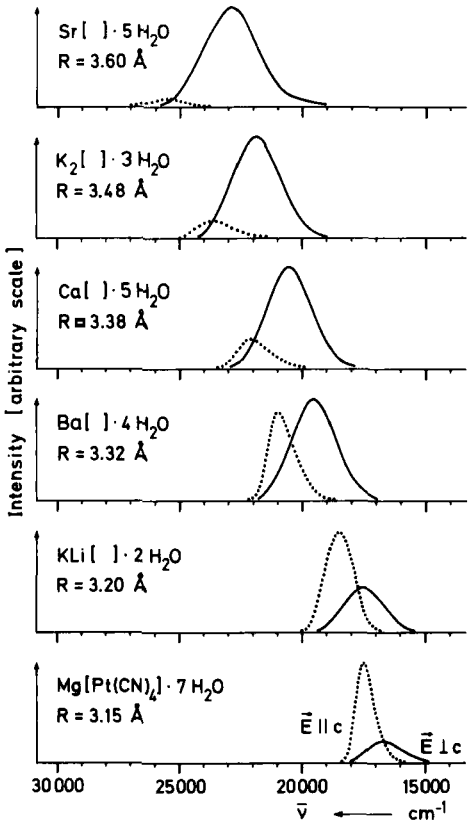

FIGURE 1. Polarized emission spectra of different tetracyanoplatinate (II) single crystals at 295 K and 1 atm. The intensities are not comparable for different compounds and the spectra are not corrected for the response of the apparatus, which is described in Reference 15 (for additional details see Reference 16). Spectral resolution: 10 cm^{-1}. The excitation energies are chosen to be about 2–3 × 10^3 cm^{-1} above the emission peak energies. Some of the compounds are discussed in detail elsewhere: BaCP,[16] KLiCP,[11] MgCP.[20]

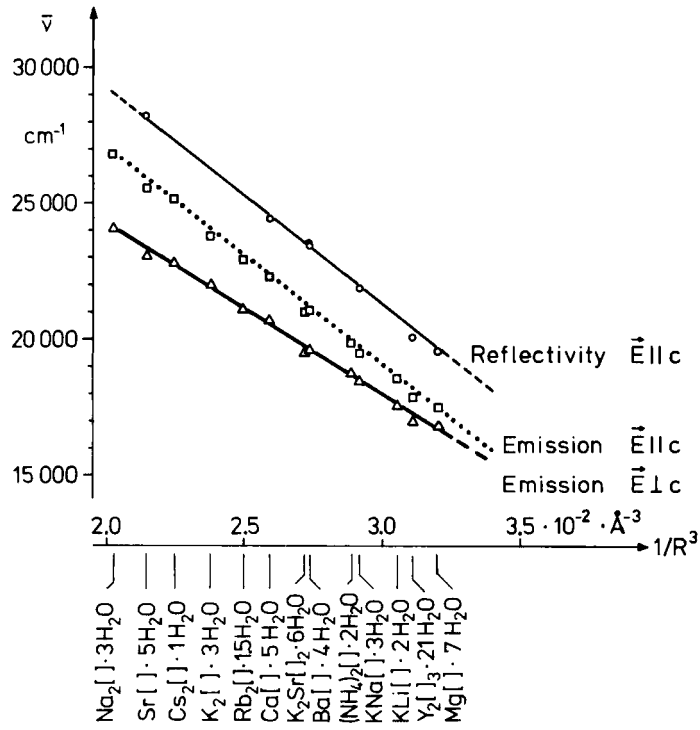

FIGURE 2. Emission and reflectivity peak energies of different $M_x[Pt(CN)_4]\cdot yH_2O$ single crystals at 295°K and 1 atm versus R^{-3}.

$(Pt\ 5d_{z^2}, 6s) \leftrightarrow (Pt\ 6p_z, CN\pi^*)$.[20,21] The emission lifetime corresponding to the $\mathbf{E} \parallel c$ transition is shorter than 10^{-8} to 10^{-9} seconds,[22] thus confirming the classification given above. The dependence of the transition energy (with $\mathbf{E} \parallel c$) on the Pt-Pt-distance R is quantitatively reproduced by one-electron calculations of the band gap energy in the framework of a two-band model (ENERGY BANDS).

Single-crystal absorption measurements[14] show that the oscillator strengths of the transitions with $\mathbf{E} \perp c$ are orders of magnitude smaller than those of the transitions with $\mathbf{E} \parallel c$. The emission lifetime for $\mathbf{E} \perp c$ is at least two orders of magnitude larger (at room temperature) than the lifetime of the parallel component.[22] Thus it is assumed that this transition is spin-forbidden and is connected with an excited triplet band that cannot be traced back simply to one dominant one-electron MO (ENERGY BANDS). The different origin of the $\mathbf{E} \perp c$ emission is also manifested by a minor red shift of the peak energies versus R^{-3} (FIGURE 2). It must be emphasized, however, that the energy difference between single-crystal absorption[14] and emission peak positions (Stokes shift) is also a function of R. This might be a consequence of R-dependent relaxation properties in the excited state that are not yet fully understood. To enlighten this effect, time-resolved emission measurements are under current investigation.[22] (See also ENERGY TRANSFER FROM $[Pt(CN)_4]^{2-}$ COLUMNS TO Sm^{3+}.)

Structural Correlation

The systematic dependence of the emission peak energies on the in-chain Pt-Pt-distance R for columnar structures of the tetracyanoplatinates(II) represents a useful correlation that may be applied to determine structural parameters.

The correlation of the emission peak energies $\bar{\nu}$ (in cm^{-1}) with the Pt-Pt-distances R (in Å) can be expressed (at 295°K) by the empirical equations[11] (FIGURE 2)

$$\mathbf{E} \,||\, c: \bar{\nu}_{||} = 42.9 \cdot 10^3 - 8.0 \cdot 10^5 R^{-3} \quad (1)$$

$$\mathbf{E} \perp c: \bar{\nu}_{\perp} = 36.8 \cdot 10^3 - 6.3 \cdot 10^5 R^{-3} \quad (2)$$

A determination of R has been achieved for the columnar structure compound KLiCP, using polarized emission peak energies. Conventional x-ray methods confirmed the result.[11]

The application of the correlation to CsCP represents an interesting example and will be discussed in more detail. The CsCP emission peak energies $\bar{\nu}_{||} = 25200\ cm^{-1}$ and $\bar{\nu}_{\perp} = 22800\ cm^{-1}$ (at 295°K) fulfill Equations 1 and 2 independently at $R = (3.56 \pm 0.02)$ Å. This value is not equal to $c/6$ ($Z = 6$) (with

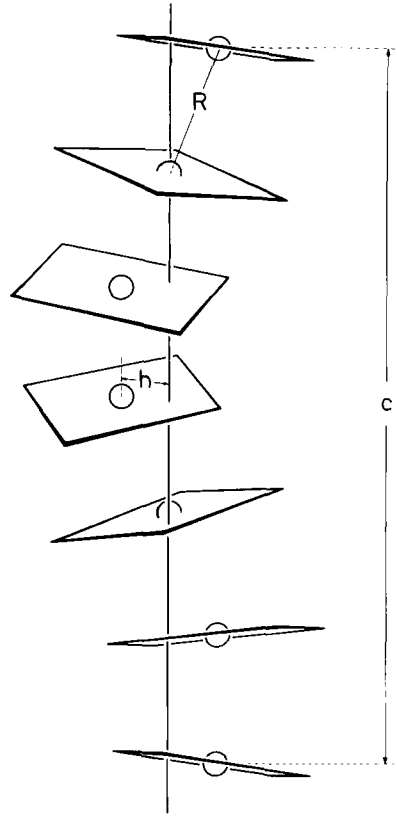

FIGURE 3. Helix of the $[Pt(CN)_4]^{2-}$ units in $Cs_2[Pt(CN)_4] \cdot H_2O$. (Space group: C_6^2-$P6_1$).[6,23]

the lattice constant c = 19.336 Å[6a]), which would be expected if the platinum atoms of the $[Pt(CN)_4]^{2-}$ units were located just on the c-axis. The first structure predictions,[6a] however, suggest a helical arrangement of the complex units lying a distance h apart from the sixfold screw axis. This implies a larger Pt-Pt-distance. If the spectroscopically determined R is assumed to be correct, it follows h = (1.50 ± 0.04) Å. Crystal structure determination confirms the values found for h and R.[6b,23] (FIGURE 3).

In spite of the lateral displacement of the $[Pt(CN)_4]^{2-}$ units, the application of Equations 1 and 2 still yields the correct Pt-Pt-distance (within limits of experimental error). This implies that the transition energies are not essentially altered. On the other hand, the energies react very sensitively to small changes of the intermolecular interaction, which is determined by the wave-function overlap. An appreciably smaller overlap would be suggested for a helix structure type unless the wavefunctions are widely spread out over the whole molecular units (although the complexes are tilted toward each other (FIGURE 3)). A calculation of the

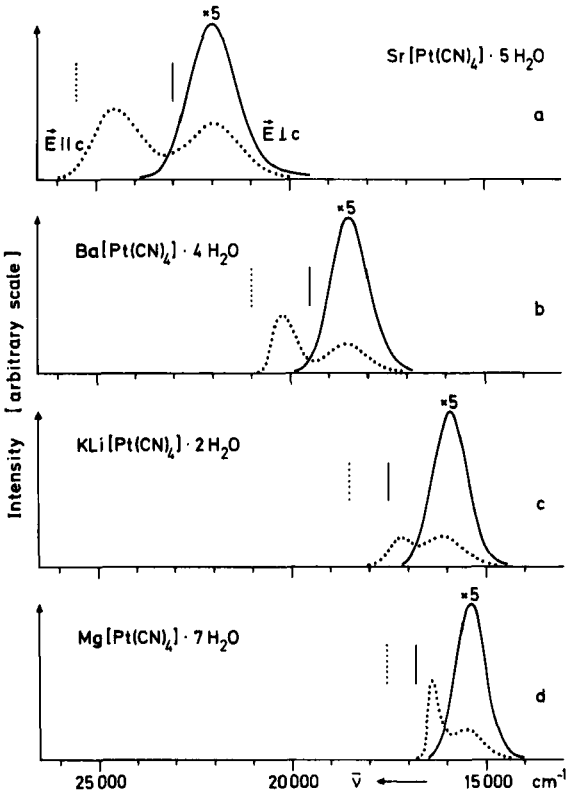

FIGURE 4. Polarized emission spectra of different tetracyanoplatinate(II) single crystals at 80°K and 1 atm. The vertical lines indicate the peak energies at 295°K ($\mathbf{E} \parallel c$: . . . , $\mathbf{E} \perp c$: ——). The $\mathbf{E} \perp c$ emission intensities have to be multiplied by a factor of 5 for comparison with the $\mathbf{E} \parallel c$-intensities. See also caption for FIGURE 1.

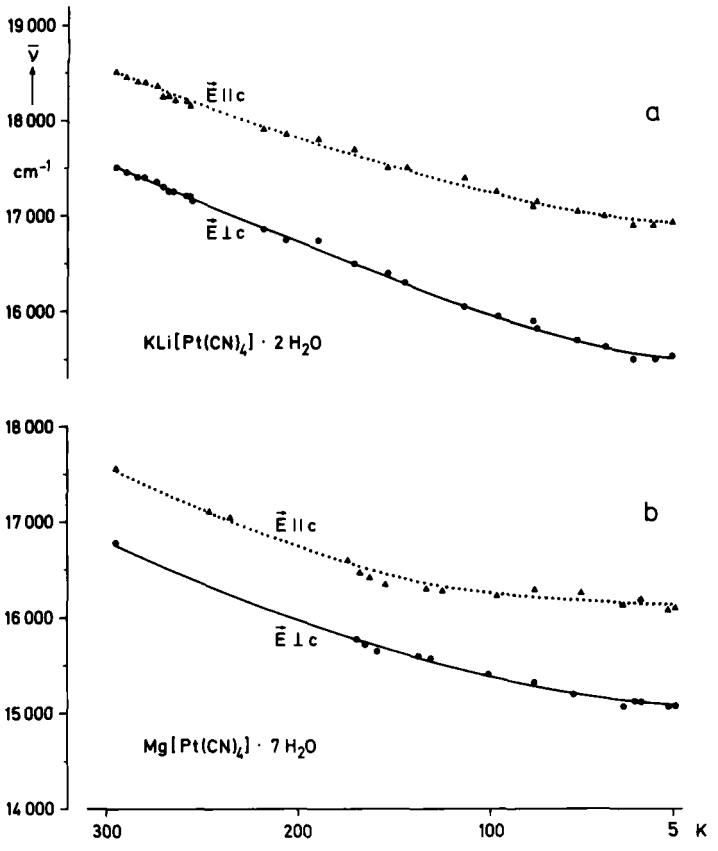

FIGURE 5. Energetic positions of the polarized single-crystal emission maxima versus temperature for KLiCP[11] and MgCP.[20]

wavefunction distribution carried out by Interrante and Messmer confirms this overall diffuseness.[24]

Low-Temperature Investigations

Temperature variation causes obvious changes of the spectroscopic properties of the tetracyanoplatinates. Thus these investigations represent a source of further information.

FIGURE 4 shows some 80°K emission spectra.* The transition energies undergo a large red shift which is also observed for the single-crystal absorption data.[14,20] FIGURE 5 reproduces the peak energies of the polarized emission versus temperature for the two compounds KLiCP[11] and MgCP.[20]

*The relative intensities of the low energetic $\mathbf{E} \parallel c$ emission peaks depend strongly on the quality of the crystals. The half-widths and peak energies are approximately the same as those of the $\mathbf{E} \perp c$ emission peaks. Therefore, the low energetic $\mathbf{E} \parallel c$ emission peaks are mainly attributed to a polarization error being about 5%.

The red shift can be attributed mainly to a large thermal contraction of the in-chain Pt-Pt-distance R leading to a temperature-dependent increase of the interaction between the molecular units and thus to a decrease of the band gap energies.[20] Recent temperature-dependent x-ray investigations for KLiCP clearly underline this interpretation. The Pt-Pt-distance R is reduced from 295°K to 80°K by $\Delta R = -(0.05 \pm 0.004)$ Å.[25]

The relative intensities of the polarized emission $I(\mathbf{E} \parallel c)/I(\mathbf{E} \perp c)$ vary strongly with temperature (compare FIGURES 1 and 4). This can be understood in a first approximation by assuming a Boltzmann distribution between the two emitting states. The lower energetic transition is spin-forbidden, whereas the higher one is fully allowed (*Spectroscopic Properties under Ambient Conditions*). Thus, as far as the rate of thermal equilibration between these two states is large compared to other processes,[26] the upper state is populated according to $\exp(-\Delta E/k_B T)$, being proportional to the relative intensities $I(\mathbf{E} \parallel c)/I(\mathbf{E} \perp c)$. ($\Delta E$ is the energy difference between the corresponding states and k_B is the Boltzmann constant.) It follows, that a reduction of the temperature T leads to a relative decrease of the upper-state emission.

The variation of the relative intensities with a change of the Pt-Pt-distance R (at constant temperature, FIGURE 1) may be explained in the same approximation. Probably ΔE increases with an increase of R. (Note: The energy difference between the emission peak energies, reproduced in FIGURE 2, has not to be equal to ΔE.)

It must be emphasized, however, that the application of the Boltzmann law is only of limited use. For example, at low temperature (5°K) the rate of the thermal equilibration between the corresponding states seems to be relatively small.[22] Consequently, the Boltzmann distribution should not be applied. A further example of a nonvalidity of this approximation is discussed in ENERGY TRANSFER FROM $[Pt(CN)_4]^{2-}$ COLUMNS TO Sm^{3+}.

Temperature reduction increases further the longest component of the emission lifetime by some orders of magnitude.[22] It also causes an appreciable half-width reduction of the emission spectra (FIGURES 1 and 4). These effects are not further discussed in this paper.

Phase Transformation in $Y_2[Pt(CN)_4]_3 \cdot 21H_2O$

Structural phase transformations that are connected with changes of the Pt-Pt-distance can be detected by monitoring the emission spectra (*Structural Correlation*). $Y_2[Pt(CN)_4]_3 \cdot 21H_2O$ (YCP) represents an informative example.[12] Between $T = 295$°K and $T > T_c = (218.5 \pm 1)$°K the YCP emission properties are equivalent to those of other tetracyanoplatinates (phase I) (FIGURE 6). *Slow* temperature reduction below T_c (≈ 10°K/h) causes a jump of the transition energies by about 10^3 cm^{-1} (phase II). Further temperature decrease leads again to typical emission properties (lower two branches of FIGURE 6, a). This behavior is attributed to a phase transformation. The columnar structure is preserved but the in-chain distance R is reduced by $\Delta R = (0.05 \pm 0.005)$ Å, determined spectroscopically from Equations 1 and 2, and also confirmed by temperature-dependent x-ray diffraction methods.[25]

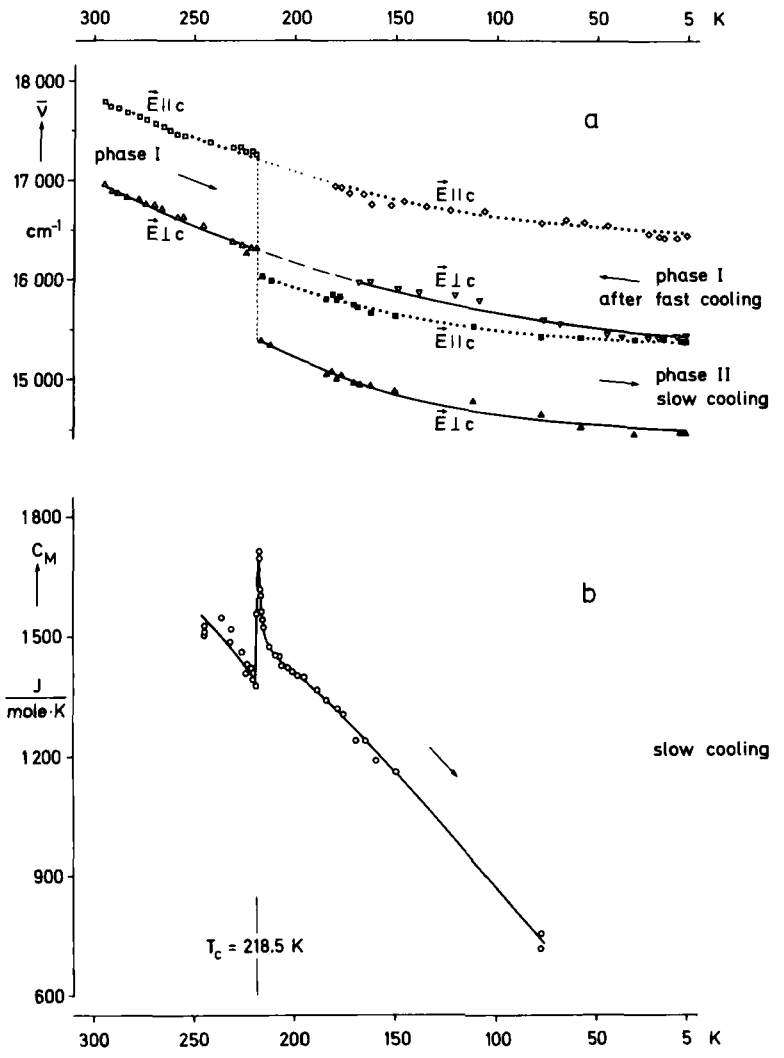

FIGURE 6. Energetic positions of the single-crystal emission maxima (a) and molar specific heat C_M (b) of $Y_2[Pt(CN)_4]_3 \cdot 21H_2O$ (YCP) versus temperature. The arrows give the direction of the temperature variation. Specific heat measurements were accomplished by a relaxation technique.[12,28]

A *fast cooling* procedure to 5°K ($\approx$30°K/min) and subsequent measurements on slowly warming up results in emission properties of the YCP compounds as if no phase transformation had occurred (upper two branches of FIGURE 6, a, including the extrapolated temperature range). It is assumed that the fast-cooling procedure leads to a supercooled phase I.[27]

The spectroscopic properties, discussed above, allow the conclusion that the

phase transformation is of first order. This is confirmed by measurements of the molar specific heat C_M, which shows a sharp peak (FIGURE 6, b), and further stated by differential thermal analysis which reveals a transition enthalpy (from phase I to phase II) of about +1500 J/mole.

The spectroscopic and the thermodynamic results lead to statements that complement each other. The spectroscopic results inform about the microscopic rearrangements, while the thermodynamic ones give information about the ensemble. The phase transformation certainly is governed by three-dimensional forces.

Polarized Emission under High Pressure

The interaction between the $[Pt(CN)_4]^{2-}$ units determining the optical transition energies depends strongly on the in-chain distance, which can be varied by chemical substitution from R = 3.67 Å to R = 3.09 Å. (TABLE 1). This method of chemical substitution, however, allows only a discontinuous "adjustment" of the Pt-Pt-distances. Application of high pressure, on the other hand, permits the adjustment of R to any intermediate value.[16] Consequently, by combination of the chemical substitution method with a high-pressure technique, a continuous "tuning" of the transition energies is possible from the near uv to the i.r.

FIGURE 7 shows the pressure-induced shift of the emission peak energies for three compounds of the tetracyanoplatinates(II).[29] The three different diagrams, all having separate pressure scales, are composed to one diagram by fitting the transition energies of the different compounds. NaCP and MgCP were selected, since to our knowledge these salts are the single-crystal compounds available with the largest and the shortest Pt-Pt-distance, respectively. R of CaCP lies just between them (TABLE 1).

The transition energies for various other tetracyanoplatinates(II) obtained under ambient conditions are also inserted in FIGURE 7. It is seen that these values fit very well within the limits of experimental error. The Pt-Pt-distances of the corresponding compounds thus lead to the upper scale.

These results demonstrate that the Pt-Pt-distance can be reduced by application of high pressure or by chemical substitution with an equivalent effect on the transition energies. Moreover, the analogy between the two methods is also valid in a first approximation concerning the relative intensities of the transitions. Consequently, this investigation indicates that the outer sphere surrounding one chain is of minor importance for the determination of the transition energies. This is the reason the correlation between pressure (lower scale of FIGURE 7) and Pt-Pt-distance (upper scale of FIGURE 7) can be given.[16] The dependence is not a linear one.

The importance of the actual crystal structure, however, clearly appears in the transition regions of NaCP and CaCP where pressure increase does not shift the emission peak energies within the limits of experimental error. Equivalent behavior has been found for BaCP at nearly the same emission peak energies.[16] The optical data do not allow a conclusive interpretation for this effect, but a reasonable assumption seems to be that phase transformations occur in these regions with no or only small changes of the Pt-Pt-distances.

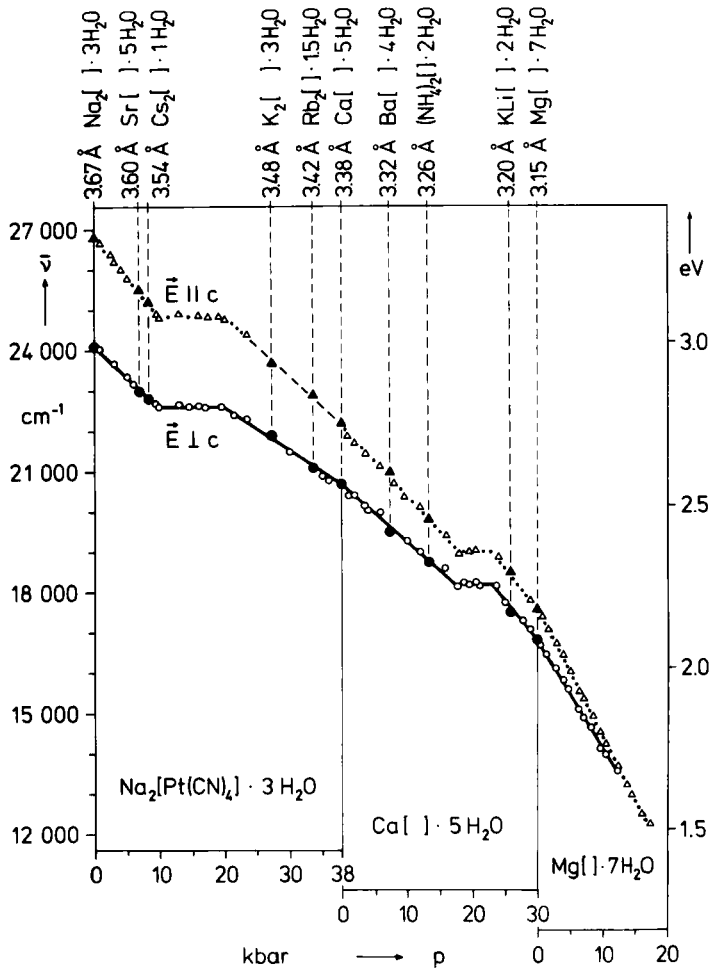

FIGURE 7. Emission peak energies for single-crystal $Na_2[Pt(CN)_4] \cdot 3H_2O$, $Ca[Pt(CN)_4] \cdot 5H_2O$, and $Mg[Pt(CN)_4] \cdot 7H_2O$ versus pressure.[29,42] The emission peak energies for various other $M_x[Pt(CN)_4] \cdot yH_2O$ salts are also inserted ($\mathbf{E} \parallel c$▲, $\mathbf{E} \perp c$●). The experimental uncertainty is about ±1 kbar and ±100 cm^{-1}.

TABLE 2 summarizes some of the results found by application of high pressure (at 295°K). It includes the peak energies of the polarized emission at 1 atm and 20 kbar, and the slopes $\Delta\bar{\nu}/\Delta p$ for p = 1 atm. These data belong to the largest values reported until the present.

ENERGY BANDS

An interpretation of essential properties of the tetracyanoplatinates can be given on the basis of a simple model. Because of the exceptional arrangement of

TABLE 2

PRESSURE-DEPENDENT ENERGY SHIFT $\Delta\bar{\nu}/\Delta p$ (1 ATM) AND EMISSION PEAK ENERGIES FOR VARIOUS TETRACYANOPLATINATES(II) AT 1 ATM AND 20 KBAR* (AT 295°K).

Compound	$\bar{\nu}_{max}$ (1 atm) [cm^{-1}]		$\bar{\nu}_{max}$ (20 kbar) [cm^{-1}]		$\frac{\Delta\bar{\nu}}{\Delta p}$ p = 1 atm [cm^{-1}/kbar]		Reference
	$E \parallel c$	$E \perp c$	$E \parallel c$	$E \perp c$	$E \parallel c$	$E \perp c$	
$Na_2[Pt(CN)_4] \cdot 3H_2O$ R = 3.67 Å	26750	24100	24800	22600	−200	−155	29
$Ca[Pt(CN)_4] \cdot 5H_2O$ R = 3.38 Å	22250	20700	19000	18200	−170	−140	29
$Ba[Pt(CN)_4] \cdot 4H_2O$ R = 3.32 Å	21000	19500	17550	16800	−280	−195	16, 30
$Mg[Pt(CN)_4] \cdot 7H_2O$ R = 3.15 Å	17550	16800	11200	—	−320	−270	42
Experimental Error	± 50		± 150		± 10%.		

*1 kbar = 10^9 dyn/cm^2 = 986.9 atm = 1020 kp/cm^2.

the molecular units in crystals with columnar structure the intermolecular coupling within every column is much stronger than the coupling between different columns. This has been stated by the high-pressure investigations (*Polarized Emission under High Pressure*). Therefore, as a rough model it seems possible to regard only a linear chain of $[Pt(CN)_4]^{2-}$-complexes.

In the case of very large intermolecular distances R, we have a system of single-oriented complex ions, without mutual coupling. The relevant one-electron states of such single complex-ions are shown schematically in FIGURE 8. It is of great importance that the ($CN\pi^*$)-states of the CN-system lie energetically in the neighborhood of the (Pt-5d/6p)-states. By coupling with the metal (Pt $6p_z$)-

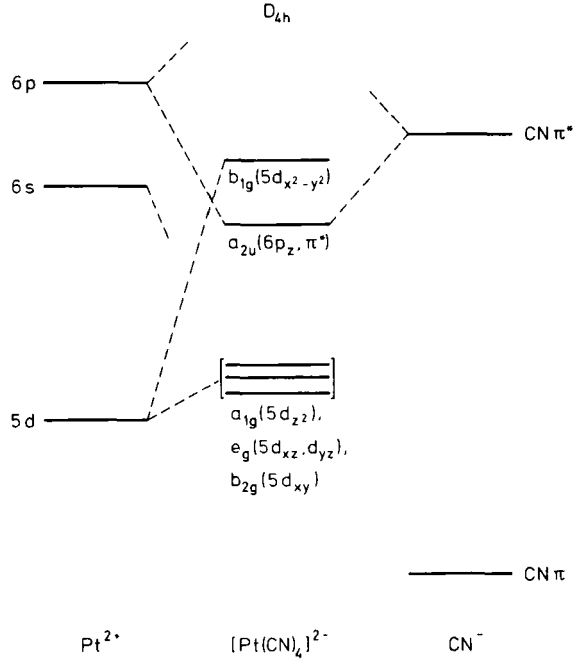

FIGURE 8. Simplified one-electron molecular orbital level diagram for $[Pt(CN)_4]^{2-}$.

orbital, a mixed molecular state (Pt $6p_z$, $CN\pi^*$) results which is located *below* the metal (Pt $5d_{x^2-y^2}$)-state, and which leads to the first excited state $^1A_{2u}$ (D_{4h}).† The ground state $^1A_{1g}$ (D_{4h}) results from the occupied (Pt $5d_{xy}$, $5d_{z2}$, $5d_{xz}$, $5d_{yz}$)-orbitals being mixed with ligand orbitals.[24,31-33] The $5d_{z^2}$ orbital may also be modified by additional Pt 6s admixtures.

If the Pt-Pt spacing R decreases, orbitals of neighboring molecular units will show increasing overlap, especially those orbitals pointing directly to the adjacent

†This is in contrast to the tetrahalogenoplatinate (II) ions, where the π^*-ligand orbitals are very high above the (Pt 5d)-levels.[14]

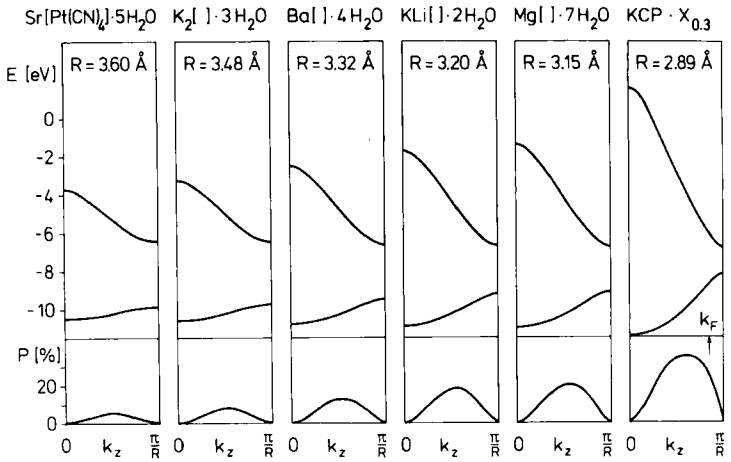

FIGURE 9. One-electron energy bands of tetracyanoplatinates with different in-chain Pt-Pt-distances R (upper part). P gives the %-contribution of the excited (Pt $6p_z$, CNπ^*) states to the valence band (Pt $5d_{z^2}$ 6s) states (lower part).[21]

metal ions. From the orbitals, cited above, (Pt $6p_z$, CNπ^*) and (Pt $5d_{z^2}$, $6s$) will have a relatively strong overlap. Consequently, a relatively broad band splitting results. For this reason the upper region of the (Pt $5d_{z^2}$, $6s$) band forms the edge of the valence band, whereas the conduction band is derived from the coupled (Pt $6p_z$, CNπ^*) states.

FIGURE 9 shows energy bands of some tetracyanoplatinates for different Pt-Pt-distances R, calculated for the two-band model in the framework of the extended Hückel theory with a modified (Pt $6p_z$), which represents the (Pt $6p_z$, CNπ^*) state and a (Pt $5d_{z^2}$[90%], $6s$[10%])-hybrid as the basis set. Details of the calculation are found in Reference 21.

The following results are obtained:

As was to be expected, with decreasing R the band splitting increases and the gap energy becomes smaller (FIGURE 9, upper part). For $k_z = \pi/R$ the calculated gap energy agrees well with the R^{-3} law obtained from optical experiments for $\mathbf{E} \parallel c$ (see FIGURE 10).

The conformity between experimental and theoretical results seems to allow an extrapolation to $R \rightarrow \infty$ ($R^{-3} \rightarrow 0$). This leads to the most prominent absorption peak of the $[Pt(CN)_4]^{2-}$ aqeuous solution,[17,18] which is assigned to correspond mainly to the (Pt $5d_{z^2}$, $6s$) $\rightarrow$ (Pt $6p_z$, CNπ^*) one-electron transition.[24,31-33,43]

An extrapolation of the experimental data to R = 2.89 Å being realized in the partially oxidized KCP · $X_{0.3}$ (FIGURE 10) leads to an energy gap of about 10^4 cm^{-1}, which corresponds to the calculated band gap energy for R = 2.89 Å. Approximately the same value has been found by Messmer and Salahub.[34]

The ($Pt\,6p_z$, $CN\pi^*$)-orbital and the ($Pt\,5d_{z^2}$, $6s$)-hybrid mix for $0 < k_z < \pi/R$, with the wave-vector k_z along the chain axis. For decreasing R the amount of ($Pt\,6p_z$, $CN\pi^*$) contribution to the ($Pt\,5d_{z^2}$, $6s$)-valence band increases and the contribution maximum shifts toward the edge of the Brillouin zone at $k_z = \pi/R$ (see bottom of FIGURE 9). The increasing contribution of ($Pt\,6p_z$, $CN\pi^*$) produces an increasing delocalization of ground state charge perpendicular to the chain axis, caused by the charge structure of the ($Pt\,6p_z$, $CN\pi^*$)-hybrid. These results have important consequences concerning three-dimensional interactions, as, for example, the interchain coupling or the properties of energy transfer to the rare-earch cations being located between the columns.

The results of the band calculations are supported by qualitative considerations in the many-electron-scheme. Starting from the many-electron states of an isolated complex ion, by coupling along the chain, the molecular singlet $^1A_{2u}$ (D_{4h}) and the molecular triplets $^3A_{2u}$, ^3E_u, $^3B_{1u}$ (primarily) generate the first excited singlet band and the lowest triplet band, respectively. Group theoretical analysis taking into account spin-orbit coupling by introducing the corresponding double group[35] (D'_{4h}) shows that the transition between the ground state and the first excited singlet band is $\mathbf{E} \parallel c$ polarized. This transition corresponds mainly to the one-electron ($Pt\,5d_{z^2}$, $6s$) $\leftrightarrow$ ($Pt\,6p_z$, $CN\pi^*$) transition. The triplet band containing admixtures of the molecular ^1E_u (D_{4h}) state (by spin orbit coupling) is allowed $\mathbf{E} \perp c$.[20]

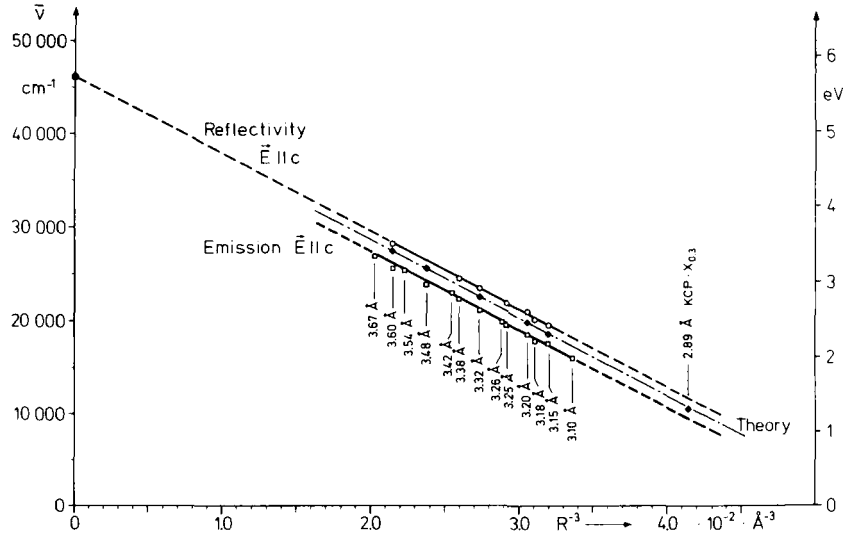

FIGURE 10. Emission and reflectivity peak energies ($\mathbf{E} \parallel c$) versus R^{-3} for various tetracyanoplatinates with different in-chain Pt-Pt-distances R at 295°K. The compounds are listed in TABLE 1. The emission peak energy at 3.10 Å is taken from Reference 42 and the point at $R^{-3} = 0$(●) represents the peak energy of the corresponding transition in solution.[17,18] The theoretical points are the band gap energies at $k_z = \pi/R$ from FIGURE 9.[21]

Because of the different charge structure of the generating molecular states, a decrease of R should produce a greater band splitting and therefore a stronger reduction of the gap energy for the singlet than for the triplet band. This is a qualitative interpretation of the different red shift of the transitions polarized $\mathbf{E} \parallel c$ and $\mathbf{E} \perp c$, respectively. The R-dependent red shift of the *emission* peak energies possibly is additionally modified by different relaxation properties in the excited states (POLARIZED SPECTROSCOPY).

ENERGY TRANSFER FROM $[Pt(CN)_4]^{2-}$ COLUMNS TO Sm^{3+}

The stacks of the tetracyanoplatinates are not isolated in the crystal. Three-dimensional interactions, not as yet studied systematically, are very important, especially the influence of the immediate surrounding on the $[Pt(CN)_4]^{2-}$ columns. For investigations of these interactions, cations having energy levels near the excited column states can yield useful information. Suitable "probe" ions are chosen out of the rare earth series (e.g. Ln = Pr^{3+}, Nd^{3+}, Sm^{3+}, Eu^{3+}). The $Ln_2[Pt(CN)_4]_3 \cdot xH_2O$ compounds also crystallize in columnar structures.[36]

The results of the spectroscopic measurements reveal important additional aspects for further investigating the LnCP systems. Radiationless energy transfer from the columns to the rare earth ions is observed. Since the excited states of the columns can be "tuned" over a large energy range by chemical substitution methods and/or applications of high pressure the tetracyanoplatinates(II) represent an exceptional donor system.

FIGURE 11 shows some results obtained for the SmCP-compound. The energy of excitation and its polarization are chosen to fit the column interband transition of very high oscillator strength ($\mathbf{E} \parallel c$). An emission from the columns (donors) *and* the Sm^{3+} ions (acceptors) is detected. Temperature reduction from 295°K to 80°K causes a red shift and a half-width reduction of the column emission and leads to an obvious enlargement of the resolution for the Sm^{3+} ion emission (FIGURE 11 a, b).

The energy transfer from the columns to Sm^{3+} represents a nonradiative process. Radiative transfer (trivial case) as well as direct acceptor excitation can be excluded, since the donor lifetime is reduced by several orders of magnitude compared to compounds with inactive cations (e.g. BaCP).[22] Another result also demonstrates that the transfer is radiationless. The acceptor ion interferes selectively with the excited column states. The relative emission intensity $I(\mathrm{E} \perp c)/I(\mathbf{E} \parallel c)$ is reduced by more than two orders of magnitude, as is seen by comparison of the 80°K SmCP spectra with the 80°K BaCP spectra. (FIGURE 11, b, and 4, b). The selective interference of Sm^{3+} with the different column states leads to the conclusion that the energy is transferred nonradiatively, mainly via the lower excited donor states of triplet character (being polarized $\mathbf{E} \perp c$).

It follows further that thermal equilibration between the excited column states (of E_u'- and A_{2u}'-character in D_{4h}') is less efficient than energy transfer to the acceptor, otherwise the relative change of the polarization would not occur. A relatively slow relaxation between the different excited column states is also indicated by investigations of time-resolved spectroscopy.[22] This possibly points to an involvement of exciton traps in the dynamics of the column emission and transfer pro-

cesses.[36] The relaxation mechanism is not fully understood; however, the results reveal the restrictions to an application of a Boltzmann distribution between the excited column states, if transfer to the acceptor represents a competitive process.

The acceptor state is not exactly known but presumably is one of the Sm^{3+} ion quartet states (FIGURE 12, a). The acceptor emission, however, can be classified to transitions from $^4G_{5/2}$ to the ^6H_J ground-state manifold.[37,38]

The mechanism of the energy transfer is not easily determined. Nevertheless, the spatial proximity of donor and acceptor favors the Dexter-exchange[39] mecha-

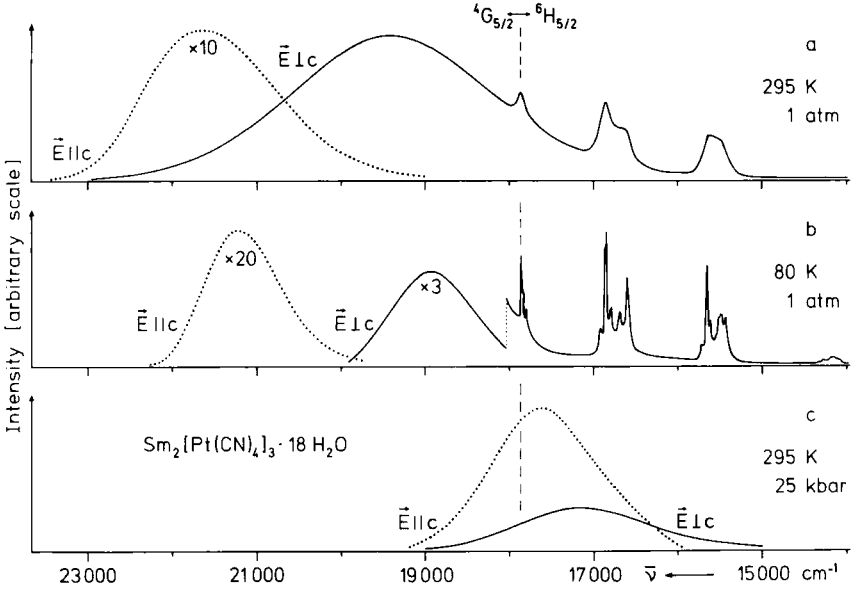

FIGURE 11. Polarized emission of single-crystal $Sm_2[Pt(CN)_4]_3 \cdot 18H_2O$ (SmCP) under different conditions.[36,42] The dashed line indicates the energy of the Sm^{3+} $^4G_{5/2} \leftrightarrow {}^6H_{5/2}$ transition. For clarity, the Sm^{3+} line-emission ($\mathbf{E} \| c$) is omitted. Note that for comparison of the intensities the spectra have to be multiplied by the factors given in the diagram. The intensities of spectra obtained at different temperature and pressure are not comparable.

nism. An inspection of crystal structures actually known[4-13] shows that nitrogen atoms of the $[Pt(CN)_4]^{2-}$ units are in the first coordination sphere of the cations. The corresponding distance is only of the order of 3 Å. Further, the $[Pt(CN)_4]^{2-}$ wave-functions are spread out over the whole complex unit with substantial amplitude even beyond the nitrogens.[24] Consequently, the wave-function overlap with the $4f$ orbitals may be considerable. Only a rough estimate of the transfer rate is possible, and in reference[36] it is pointed out that the exchange transfer presumably predominates the Coulomb transfer mechanism. Further, it is shown that the Wigner spin selection rules[40] for an exchange transfer from the excited triplet column state to the quartet Sm^{3+} state are fulfilled.

Energy transfer from the columns to the rare earth ions can be detected only if the energetic position of the emitting acceptor states is low enough that even a phonon-assisted back-transfer to the donor states can be excluded. This has been established not only for SmCP but also for various other compounds (e.g. EuCP, PrCP, and TbCP).[36] Crosby *et al.* discussed this rule investigating a large series of rare earth chelates.[41] Consequently, it seems to be possible that the Sm^{3+} emis-

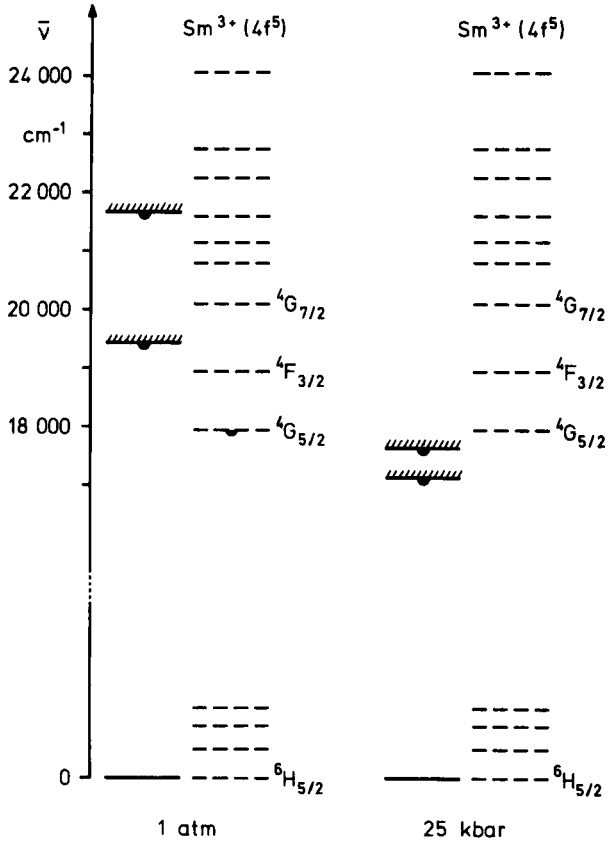

FIGURE 12. Energy level schemes for $Sm_2[Pt(CN)_4]_3 \cdot 18H_2O$ at 1 atm and 25 kbar at 295°K. The shaded bars represent the emission maxima of the $[Pt(CN)_4]^{2-}$ columns. The dashed lines represent the Sm^{3+} levels.[37,38] The black half circles indicate emitting states.

sion (of SmCP) can be quenched if the excited column states are shifted to lower energy. This is demonstrated in FIGURE 11, c.[42] Application of 25 kbar results in a red shift of the column states by several thousand wave-numbers and leads to the expected disappearance of the Sm^{3+} emission. Connected with this quenching the relative intensity of the polarized column emission $I(\mathbf{E} \perp c)/I(\mathbf{E} \parallel c)$ is changed to the same ratio as if the cations were inactive.

In FIGURE 12 the relevant energy-level diagram for SmCP under ambient con-

ditions is compared to that under 25 kbar. The disappearance of the Sm^{3+} emission seems to be connected with a change of the spectral overlap integral[39] between the $\vec{E} \perp c$ donor-emission and $^4F_{3/2}$ acceptor-absorption.[36]

Conclusion

The tetracyanoplatinates(II) represent an exceptional class of compounds due to the arrangement of the $[Pt(CN)_4]^{2-}$ units in quasilinear stacks. The special structure leads to very strong intermolecular interactions in the direction of the columns and relatively weak interchain interactions. As a consequence of this structure type, the physical properties are very anisotropic. Methods of polarized spectroscopy with special emphasis on polarized emission spectroscopy represent adequate techniques for studying these compounds. The transitions follow different selection rules and can be classified group-theoretically. The transition energies are determined essentially by one parameter, the in-chain Pt-Pt-distance. The energy dependence can be reproduced quantitatively (for the highly allowed transition with $\mathbf{E} \parallel c$) by one-electron band structure calculations. These, as well as spectroscopic predictions, permit the determination of band-gap energy for the partially oxidized tetracyanoplatinate (e.g. $K_2[Pt(CN)_4]Br_{0.3} \cdot 3.2H_2O$).

It has further been demonstrated that the in-chain Pt-Pt-distance can be adjusted by chemical substitution (cation exchange) or application of high pressure having an equivalent effect on the energies of the electronic transitions. Regarding these properties, the compounds behave as being pseudoone-dimensional. Of importance is that transition energies can be "tuned" almost continuously from the near uv to the near i.r.. The possibility of tuning the excited column states may imply some future technical applications.

Interactions of the columns with their immediate surroundings have been studied by incorporation of "probe" ions selected of the series of the rare earth ions (Ln^{3+}). For $Sm_2[Pt(CN)_4]_3 \cdot 18H_2O$ (SmCP), it could be shown that a radiationless energy transfer from the columns (donors) to SM^{3+} (acceptor) occurs. The investigations reveal that the energy transfer rate is much larger than the thermal relaxation rate between the excited column states. This possibly points to an involvement of exciton traps in the dynamics of the column-emission process.

The main importance of the LnCP compounds, however, does not seem to be the "probing" effect of the Ln^{3+} ions but the new possibilities existing for energy transfer investigations with *tunable donor states*. Thus it has been shown for SmCP that the high pressure-induced red shift of the donor (column) states leads to a quenching of the SM^{3+} emission.

References

1. Interrante, L. V., Ed. 1974. Extended Interactions Between Metal Ions in Transition Metal Complexes. ASC Symposium. Washington, D.C.
2. Keller, H. J., Ed. 1975. Low-Dimensional Cooperative Phenomena. Plenum Press. New York, N.Y.
3. Miller, J. S. & A. J. Epstein. 1976. Prog. Inorg. Chem. **20:** 1.
4. Moreau-Colin, M. L. 1972. Struct. Bonding **10:** 167.
5. Krogmann, K. & D. Stephan. 1968. Z. Anorg. Allgem. Chem. **362:** 290.

6a. Otto, H. H., W. Holzapfel, H. Yersin & G. Gliemann. 1976. Z. Naturforsch. Teil b. **31:** 528.

6b. OTTO, H. H., SCHULZ, K. H. THIEMANN, H. YERSIN & G. GLIEMANN. 1977. Z. Naturforsch. Teil b. **32:** 127.
7. WASHECHECK, D. M., S. W. PETERSON, A. H. REIS & J. M. WILLIAMS. 1976. Inorg. Chem. **15:** 74.
8. KOCH, T. R., P. L. JOHNSON & J. M. WILLIAMS. 1977. Inorg. Chem. **16:** 640.
9. MAFFLY, R. L., P. L. JOHNSON & J. M. WILLIAMS. 1977. Acta Cryst. **B33:** 884.
10. MOREAU-COLIN, M. L. 1968. Bull. Soc. Mineral. Cristallogr. **91:** 332.
11. HOLZAPFEL, W., H. YERSIN, G. GLIEMANN & H. H. OTTO. 1978. Ber. Bunsenges. Phys. Chem. **82:** (Heft 2). In press.
12. YERSIN, H., G. GLIEMANN & H.-S. RÄDE. 1978. Chem. Phys. Lett. In press.
13. KROGMANN, K. & H. D. HAUSEN. 1968. Z. Anorg. Allgem. Chem. **358:** 67.
14. TUSZYNSKI, W. & G. GLIEMANN. Unpublished.
15. YERSIN, H. & G. GLIEMANN. 1972. Meßtechnik **80:** 99.
16. STOCK, M. & H. YERSIN. 1976. Chem. Phys. Lett. **40:** 423.
17. YERSIN, H. & G. GLIEMANN. 1975. Ber. Bunsenges. Phys. Chem. **79:** 1050.
18. DAY, P. 1975. J. Am. Chem. Soc. **97:** 1588, and Ref. 1, p. 234.
19. MONCUIT, C. & H. POULET. 1962. J. Phys. Rad. **23:** 353.
20. YERSIN, H. & G. GLIEMANN. 1975. Z. Naturforsch. **30b:** 183.
21. YERSIN, H., G. GLIEMANN & U. RÖSSLER. 1977. Solid State Comm. **21:** 915.
22. GERHARDT, V. & W. v. AMMON *et al.* (Regensburg.) Unpublished.
23. GLIEMANN, G., W. HOLZAPFEL, H. H. OTTO & H. YERSIN. Inorg. Chim. Acta. Submitted.
24a. INTERRANTE, L. V. & R. P. MESSMER. Ref. 1. p. 382.
24b. INTERRANTE, L. V. & R. P. MESSMER. 1974. Chem. Phys. Lett. **26:** 225.
25. DANIELS, W. Diplomarbeit (Regensburg.) Unpublished.
26. YERSIN, H., H. OTTO & G. GLIEMANN. 1974. Theor. Chim. Acta **33:** 63.
27. GREEN, H. S. & C. A. HURST. 1964. Order-Disorder Phenomena. Wiley Interscience. New York, N.Y.
28. RÄDE, H.-S. 1975. Meßtechnik **83:** 230.
29. STOCK, M., I. HIDVEGI *et al.* (Regensburg.) Unpublished.
30. YERSIN, H. & M. STOCK. 1976. Proceedings XVIII[th] ICCC: 103. Hamburg, Germany.
31. PIEPHO, S. B., P. N. SCHATZ & A. J. MCCAFFERY. 1969. J. Amer. Chem. Soc. **91:** 5994.
32. ISCI, H. & W. R. MASON. 1975. Inorg. Chem. **14:** 905.
33. MARSH, D. G. & J. S. MILLER. 1976. Inorg. Chem. **15:** 720.
34. MESSMER, R. P. & D. R. SALAHUB. 1975. Phys. Rev. Lett. **35:** 533.
35. SCHLÄFER, H. L. & G. GLIEMANN. 1969. Basic Principles of Ligand Field Theory. Wiley Interscience. New York, N.Y.
36. YERSIN, H. 1976. Ber. Bunsenges. Phys. Chem. **80:** 1237; J. Chem. Phys. Submitted.
37. DIEKE, G. H. 1968. Spectra and Energy Levels of Rare Earth Ions in Crystals. Wiley Interscience. New York, N.Y.
38. STEIN, G. & E. WÜRZBERG. 1975. J. Chem. Phys. **62:** 208.
39. DEXTER, D. L. 1953. J. Chem. Phys. **21:** 836.
40. LAMOLA, A. A. 1969. *In* Energy Transfer and Organic Photochemistry. A. A. Lamola and N. J. Turro, Eds.: 17. Wiley Interscience. New York, N.Y.
41. CROSBY, G. A., R. E. WHAN & R. M. ALIRE. 1961. J. Chem. Phys. **34:** 743.
42. YERSIN, H. & M. STOCK. Submitted for publication.
43. COWMAN, C. D. & H. B. GRAY. Inorg. 1976. Inorg. Chem. **15:** 2823.

DISCUSSION

PETER DAY: There are two different starting points from which one could set out to describe the electronic structure of molecular materials. One is the route

that you took in your tight-binding one-electron band-structure calculation. The other approach for a molecular solid would be to assume that there was essentially zero electron exchange between the constituent molecules, and then discuss the optical properties in terms of tightly bound excitons. Have any of the experiments that you have described actually enabled one to distinguish which is the better model for these substances? The most direct evidence that you could expect to have, at least for the excited states, would be if one detected photoconductivity. We attempted to detect photoconductivity, and to a very good approximation did not find any.

YERSIN: The electronic properties of the tetracyanoplatinates(II) along the stacking direction presumably lie in between these extreme limits. However, the wavefunctions overlap in chain direction is large, leading to delocalized Bloch-functions. The band-structure calculation based on this model quantitatively describes the transition energies for $\mathbf{E} \parallel c$. The measurement of photoconductivity can be obscured by many effects. Possibly trapping effects prevent the detection of photocurrents.

JACK WILLIAMS: The disodium tetracyanoplatinate trihyrate has a zig-zag chain and three different platinum-platinum separations. Which separation do you use in your calculations?

YERSIN: In most cases the emission comes from the lowest excited states, and this would lead to the shortest metal-metal distance. However, the error bars for the spectroscopic metal-metal distance determination is rather large in the corresponding UV emission range.

JERRY TORRANCE: If you extrapolate your energy as a function $1/R^3$ to infinite separation, you get an energy for that transition. How does that compare to what you find in solution?

YERSIN: The formal extrapolation leads to the energy value of the corresponding transition observed in solution.